ISSN 0006-3509, Biophysics, 2016, Vol. 61, No. 6, pp. 942–949. © Pleiades Publishing, Inc., 2016.
Original Russian Text © D.V. Bagrov, N. Voskoboynikova, G.A. Armeev, W. Mosslehy, G.S. Gluhov, T.T. Ismagulova, A.Y. Mulkidjanian, M.P. Kirpichnikov, H.-J. Steinhoff, K.V. Shaitan, 2016, published in Biofizika, 2016, Vol. 61, No. 6, pp. 1139–1148.

CELL BIOPHYSICS

Characterization of Lipodisc Nanoparticles Containing Sensory Rhodopsin II and Its Cognate Transducer from *Natronomonas pharaonis*[1]

D. V. Bagrov[a, *], N. Voskoboynikova[b, **], G. A. Armeev[a], W. Mosslehy[b], G. S. Gluhov[a], T. T. Ismagulova[a], A. Y. Mulkidjanian[b], M. P. Kirpichnikov[a], H.-J. Steinhoff[b], and K. V. Shaitan[a]

[a] *Department of bioengineering, Faculty of Biology, Lomonosov Moscow State University, Moscow, 119234 Russia*
[b] *Department of Physics, University of Osnabrück, Osnabrück, 49069 Germany*
**e-mail: dbagrov@gmail.com*
***e-mail: nvoskobo@uni-osnabrueck.de*
Received February 4, 2016

Abstract—We describe the preparation and properties of lipodisc nanoparticles – lipid membrane fragments with a diameter of about 10 nm, stabilized by amphiphilic synthetic polymer molecules. We used the lipodisc nanoparticles made of *Escherichia coli* polar lipids and compared lipodisc nanoparticles that contained the photosensitive protein complex of the sensory rhodopsin with its cognate transducer from the halobacterium *Natronomonas pharaonis* with empty lipodisc nanoparticles that contained no protein. The lipodisc nanoparticles were characterized by dynamic light scattering, transmission electron microscopy and atomic force microscopy. We found that the diameter of lipodisc nanoparticles was not affected by incorporation of the protein complexes, which makes them a prospective platform for single-molecule studies of membrane proteins.

Keywords: membrane proteins, rhodopsin, lipodisc nanoparticles, transmission electron microscopy, atomic force microscopy

DOI: 10.1134/S0006350916060063

INTRODUCTION

In recent years, new methods of structure analysis have emerged, including the X-ray free electron lasers (XFEL) based techniques [1–4] and novel approaches of hydrophobic structure crystallization [5, 6]. The development of these methods and approaches is complicated and involves aspects associated with sample preparation, structure stabilization, conducting the experiments, as well as processing of X-ray scattering patterns to obtain information about the spatial structure of the macromolecules [7–10]. The choice of the optimal molecular or supramolecular composition for structural and dynamic experiments also becomes relevant. Lipid nanoparticles (nanodiscs and lipodiscs) are potent containers (carriers) for single molecule experiments with membrane proteins.

Traditionally, membrane proteins are stabilized in detergent solution or liposomes; in some cases, bicelles (particles consisting of two types of lipids with different curvature) [11] and planar lipid layers are used [12]. Both nanodiscs and lipodisc nanoparticles contain patches of a lipid bilayer with a diameter of ~10 nm. In nanodiscs, the lipid bilayer is encircled by amphiphilic proteins [13, 14], in lipodisc nanoparticles it is held together by amphiphilic synthetic polymers [15–23]. The amphiphilic protein of nanodiscs is usually the membrane scaffold protein (MSP), a recombinant analogue of lipoprotein A [14], whereas the amphiphilic polymer of the lipodisc nanoparticles is the styrene maleic acid (SMA) copolymer [23]. The MSP and SMA molecules protect the hydrophobic edges of the discs from contact with water. Thereby the central part of the disc, which is stable in an aqueous environment, can host a membrane protein. Thus, lipodisc nanoparticles and nanodiscs are regarded as prospective containers for individual (single) membrane proteins.

Nanodiscs are widely used to keep membrane proteins water-soluble during experimental structure studies by NMR [24–26], cryo-electron microscopy [27], or EPR [28]. Lipodisc nanoparticles containing individual protein molecules are less popular and relatively poorly understood. However, the advantage of the lipodisc nanoparticles is that they require no

[1] The article was translated by the authors.

detergents during assembly and thus preserve natural lipid microenvironment, which in some cases may be important to maintain the native conformation of a protein [21].

In this paper we studied the lipodisc nanoparticles consisting of the polar lipid membranes from *Escherichia coli* and stabilized by SMA copolymer. We inserted a photoactive membrane protein into the lipodisc nanoparticles and compared the size of the loaded and the empty nanoparticles.

We have chosen the membrane-embedded photoactive sensory rhodopsin II (*Np*SRII) from the archaeal halobacterium *Natronomonas pharaonis*. The protein, which is structurally and functionally related to the light-driven ion pumps bacteriorhodopsin and halorhodopsin, mediates the photophobic response of halobacteria to harmful blue light [29–31]. In membranes, *Np*SRII forms a tightly associated complex with a cognate transducer protein *Np*HtrII (halobacterial transducer of rhodopsins) [32] with a stoichiometry of 2 : 2 [33]. After light activation of *Np*SRII, the signal is transferred to *Np*HtrII that transmits the signal further to the intracellular signaling pathway which modulates the swimming behavior of the cell. The previous studies of the photoreceptor/transducer complex, *Np*SRII/*Np*HtrII, in the lipid model system were mostly performed using mesoscopic purple membrane lipid (PML) patches. Thereby, the possible clustering of *Np*SRII/*Np*HtrII complexes in PML [34] made it virtually impossible to explore the functional properties of a single *Np*SRII/*Np*HtrII complex.

In this paper, we studied the properties of lipodisc nanoparticles that contained membrane polar lipids from *Escherichia coli* and were stabilized by SMA copolymer. We inserted a *Np*SRII/*Np*HtrII$_{157}$ protein complex with the transducer truncated at position 157 and compared the size and shape of protein-loaded lipodisc nanoparticles with those of empty lipodisc nanoparticles. The lipoprotein nanoparticles were characterized by dynamic light scattering (DLS), transmission electron microscopy (TEM), and atomic force microscopy (AFM).

MATERIALS AND METHODS

NpSRII/NpHtrII$_{157}$ Expression and Purification

For purification purposes, all proteins had a C-terminal 6xHis-tag. The *Np*SRII–His and *Np*HtrII$_{157}$–His (transducer construct that was truncated at position 157) were expressed in *E. coli* BL21 (DE3) according to [35–37] with minor modifications. Briefly, cells were grown in LB medium (with 50 mg/mL kanamycin, at 37°C) to an optical density OD_{580} of 0.8–1.0, and overexpression was induced by 0.5 mM IPTG. After induction, the cells were incubated for 3 h at 37°C. The cells were harvested (15 min, 3000 *g*, SLA-3000), washed and then resuspended in the cell wash buffer (150 mM NaCl, 25 mM NaP_i, 2 mM EDTA, pH 8.0; 1/100 culture volume), and disrupted by sonication (Branson Sonifier 250). The membrane fraction was isolated by centrifugation (50000 *g*, 1 h, 4°C) and membrane proteins were solubilized overnight (4°C) in buffer A that contained 300 mM NaCl, 50 mM NaP_i, pH 8.0, 2% (w/v) *n*-dodecyl-β-D-maltoside (DDM). The solubilized membrane proteins were isolated by centrifugation (50000 *g*, 1 h, 4°C) and incubated (2 h) with the equilibrated (buffer B: 300 mM NaCl, 50 mM NaP_i, pH 8.0, 0.05% (w/v) DDM) Ni-NTA superflow (Quiagen) material in the presence of 15 mM imidazole. Unspecifically bound proteins were removed by washing with buffer B containing 30 mM imidazole. The His-tagged proteins were eluted with buffer B containing 200 mM imidazole. From the fractions containing the desired protein, imidazole was removed by dialysis against 500 mM NaCl, 10 mM Tris pH 8.0, 0.05% (w/v) DDM. If not used directly for reconstitution, protein solutions were stored at −80°C.

SMA Copolymer Preparation

SMA copolymer with a styrene/maleic acid ratio of 3 : 1 (M_W 9500 Da, supplied as an aqueous sodium salt solution SMA 3000 HNa) was kindly provided as a gift by Cray Valley (Exton, PA). A 5% (w/v) solution of SMA, which was extensively dialysed against buffer C (10 mM Tris-HCl pH 8, 150 mM NaCl), was used for reconstitution studies.

Preparation of Liposomes and Proteoliposomes

The polar lipid extract of *Escherichia coli* membranes in chloroform was purchased from Avanti Polar Lipids, Inc. (Alabaster, AL, USA). Lipids were quantitatively transferred to a glass flask, and chloroform was removed by drying under nitrogen flow. After evaporation of chloroform, the lipid film was dried under vacuum for at least 1 h, then hydrated in buffer C by stirring for about 30 min. The hydrated lipid suspension was then subjected to 5 freeze/thaw cycles and, if not used directly, stored as aliquots at −80°C. Subsequently, before reconstitution, the lipid suspension obtained was passed at least 11 times through the Mini-Extruder (Avanti Polar Lipids, Inc.) using polycarbonate membranes (Whatman) with a pore size diameter of 400 or 200 nm.

The reconstitution of the complex of *Np*SRII and *Np*HtrII$_{157}$ into liposomes was performed by using SM-2 Bio-Beads (Bio-Rad Laboratories, München, Germany). Firstly, *Np*SRII and *Np*HtrII$_{157}$ were mixed at a 1 : 1 molar ratio and incubated for 1 h at room temperature. Subsequently, membrane proteins were mixed with liposomes at a molar protein/lipid ratio of 1 : 172. For extracting DDM, the assembly mixture was incubated with Bio-Beads (50 mg of beads/mg of detergent) for 16 h at 4°C. Bio-Beads were prewashed extensively with methanol and water. Proteoliposomes were pelleted by centrifugation (15 min, 15800 *g*, 4°C) and then resuspended in buffer C.

Preparation of the Empty and Loaded Lipodisc Nanoparticles

To form the lipodisc nanoparticles, with and without *Np*SRII/*Np*HtrII$_{157}$, a 5% (w/v) solution of SMA copolymer in buffer C was added dropwise to a proteoliposome suspension or a liposome suspension, respectively, to get a final lipid-to-SMA ratio of 1 : 2.5 (w/w); after that the assembly mixture was allowed to equilibrate for 1 h at room temperature and then for 16 h at 4°C. The resulting samples, which contained *Np*SRII/*Np*HtrII$_{157}$–lipodisc nanoparticles or empty lipodisc nanoparticles, respectively, were centrifuged (50000 *g*; 30 min; 4°C) to remove non-solubilized material.

Dynamic Light Scattering (DLS) Measurements

DLS measurements were performed on a Zetasizer Nano ZS (Malvern Instruments, Worcestershire, United Kingdom) at 25°C. Data represent the average of three sets of 14 subruns of 10 s each. The particle size distribution was obtained by using ZETASIZER software package Ver. 7.02. under the assumption that lipodisc nanoparticles were spherically shaped.

Size Measurements by Transmission Electron Microscopy (TEM)

For TEM imaging, a solution of the lipodisc nanoparticles (either empty or with the *Np*SRII/*Np*HtrII$_{157}$ complex) was deposited on Ted Pella grids treated with a glow discharge device Emitech K100X. A drop of solution was incubated for 1–2 min, then treated with 1% uranyl acetate for 1 min and dried. Images were obtained on JEM-2100 (Jeol, Japan) transmission electron microscope operated at 200 kV. The lipodisc nanoparticles were analyzed with ImageJ software [38].

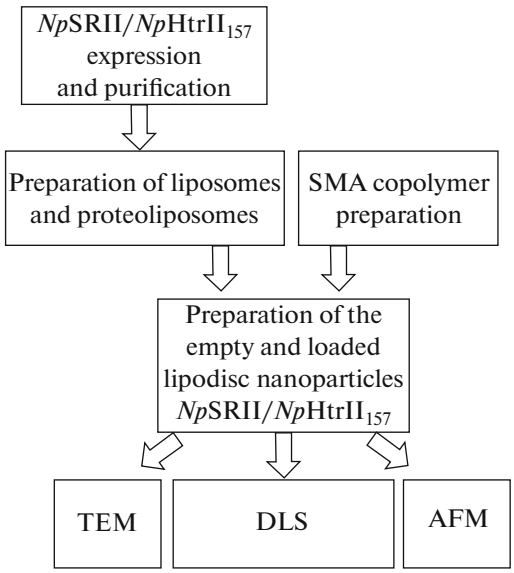

Fig. 1. The general scheme of the experiments.

Size Measurements by Atomic Force Microscopy (AFM)

For AFM imaging, a solution of the lipodisc nanoparticles (either empty or with the *Np*SRII/*Np*HtrII$_{157}$ complex) was diluted by the buffer containing 10 mM TrisHCl, pH 8, 150 mM NaCl, 10 mM $MgCl_2$ and deposited on freshly cleaved mica. The solution was incubated for 5 min, then mica was washed with 1 mL of buffer and transferred to the AFM liquid cell. The measurements were carried out on a Solver PRO microscope (NT-MDT, Russian Federation) operating in semicontact mode in buffer. We used MSCT-AUHW cantilevers, the obtained images were processed with FemtoScan Online software.

RESULTS AND DISCUSSION

The general scheme of the experiments carried out in this article, is presented in Fig. 1. The experiments included the isolation and purification of the protein complex *Np*SRII/*Np*HtrII$_{157}$, the formation of liposomes and proteoliposomes, the formation of two types of the lipodisc nanoparticles: the empty (control) ones and the ones containing *Np*SRII/*Np*HtrII157, and the investigation of the produced lipodisc nanoparticles by the three analytical methods.

Proteins *Np*SRII and *Np*HtrII$_{157}$ from *N. pharaonis* were purified using a heterologous expression in *E. coli* cells followed by purification by affinity chromatography which was performed on a metal-chelate Ni-NTA sorbent (see Materials and Methods). The complex *Np*SRII/*Np*HtrII$_{157}$ (at a molar ratio of 1 : 1) was

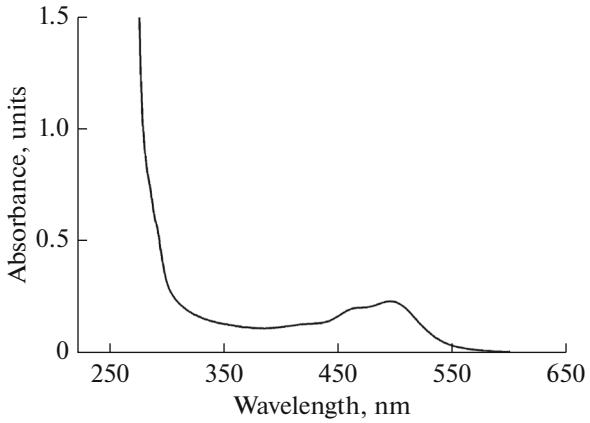

Fig. 2. Absorption spectrum of *Np*SRII/*Np*HtrII$_{157}$ complex in lipodisc nanoparticles.

inserted into the liposomes from *E. coli* membrane polar lipids, and the resulting proteoliposomes were exposed to the SMA copolymer at a weight lipid-to-polymer ratio of 1 : 2.5.

Figure 2 shows the absorption spectrum of the solution of lipodisc nanoparticles containing the *Np*SRII/*Np*HtrII$_{157}$ complex. The absorption maximum at 500 nm, being due to the absorption of the chromophore group, retinal, in the *Np*SRII, indicates the presence of the protein in the sample. The dissociation constant K_d of the heterogeneous complex *Np*SRII/*Np*HtrII$_{157}$ was shown to be 240 nM [39]. The concentration of sensory rhodopsin in the sample was about 9 μM; its volume concentration in the lipid phase had to be several orders of magnitude higher. Accordingly, the *Np*SRII and *Np*HtrII$_{157}$ should be present in the lipodisc nanoparticles as a complex.

We used TEM to measure the size distributions of the lipodisc nanoparticles. Figure 3 shows the images of empty lipodisc nanoparticles and lipodisc nanoparticles with the *Np*SRII/*Np*HtrII$_{157}$ complex. The size distributions are plotted in Fig. 4. Each of the distributions was obtained by measuring 200 lipodisc nanoparticles, each particle was measured twice (amount of sampling $N = 400$). The distributions have single maxima but are not Gaussian. According to the Mann-Whitney test they are not significantly different, meaning that the empty lipodisc nanoparticles and the lipodisc nanoparticles containing the *Np*SRII/*Np*HtrII$_{157}$ complex have the same average size of 15 ± 3 nm. The majority of lipodisc nanoparticles are 12.8–13 nm in diameter. This value is in perfect agreement with the results obtained by the other authors [15, 23]. We did not observe a bimodal size distribution [23].

Lipodisc nanoparticle preparations were analysed by dynamic light scattering (DLS) measurements. We obtained the intensity distributions of particle sizes for the *Np*SRII/*Np*HtrII$_{157}$-loaded and the empty lipodisc nanoparticles. Both distributions had two peaks (Fig. 5). The intensity-based mean diameter was approximately 10 nm for both types of nanoparticles. The peak near 150–220 nm was attributed to aggregates of lipid and SMA. They are larger than single lipodisc nanoparticles so they caused more intense scattering. However, they are relatively few in numbers, as they were difficult to find by TEM. A similar distribution was shown in [15]. The DLS-obtained values were smaller than those obtained with the TEM technique (15±3 nm). The difference might be attributed to the different physical properties that were actually measured, namely the hydrodynamic diame-

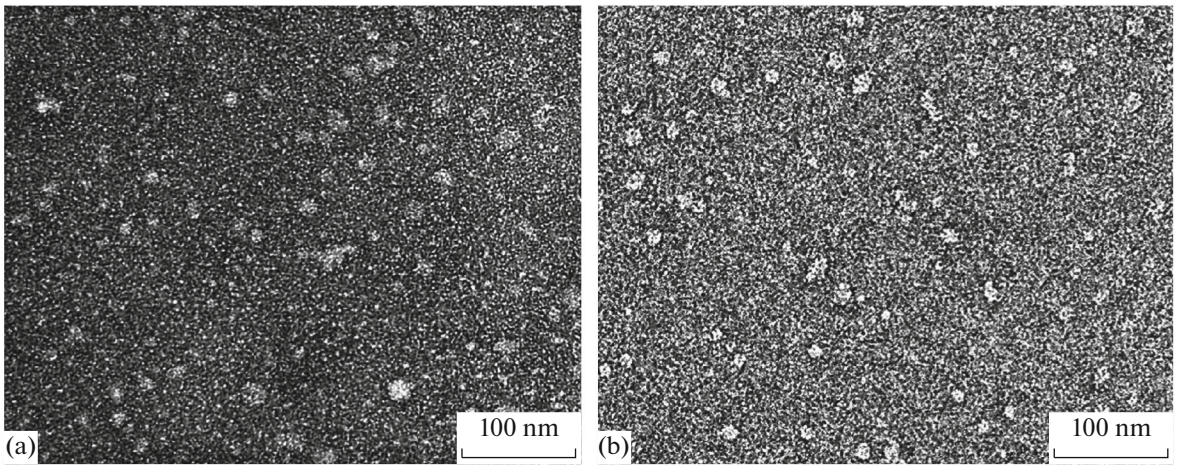

Fig. 3. TEM images of the empty lipodisc nanoparticles (left) and the lipodisc nanoparticles containing the *Np*SRII/*Np*HtrII$_{157}$ complex (right).

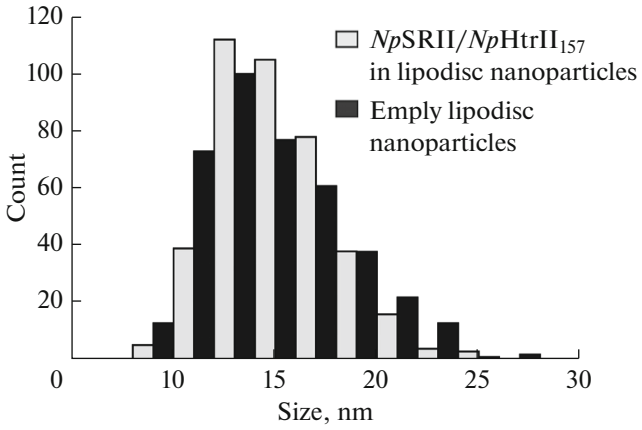

Fig. 4. Size distributions of the empty lipodisc nanoparticles and the lipodisc nanoparticles with the *Np*SRII/*Np*HtrII$_{157}$ complex based on the TEM data.

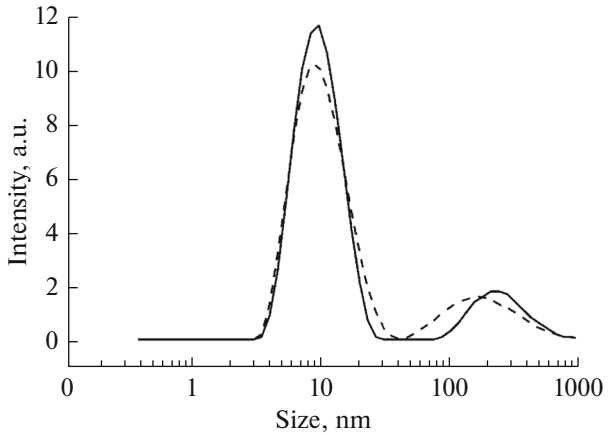

Fig. 5. Size distributions of the empty lipodisc nanoparticles (solid line) and the lipodisc nanoparticles with the *Np*SRII/*Np*HtrII157 complex (dotted line) based on the DLS data.

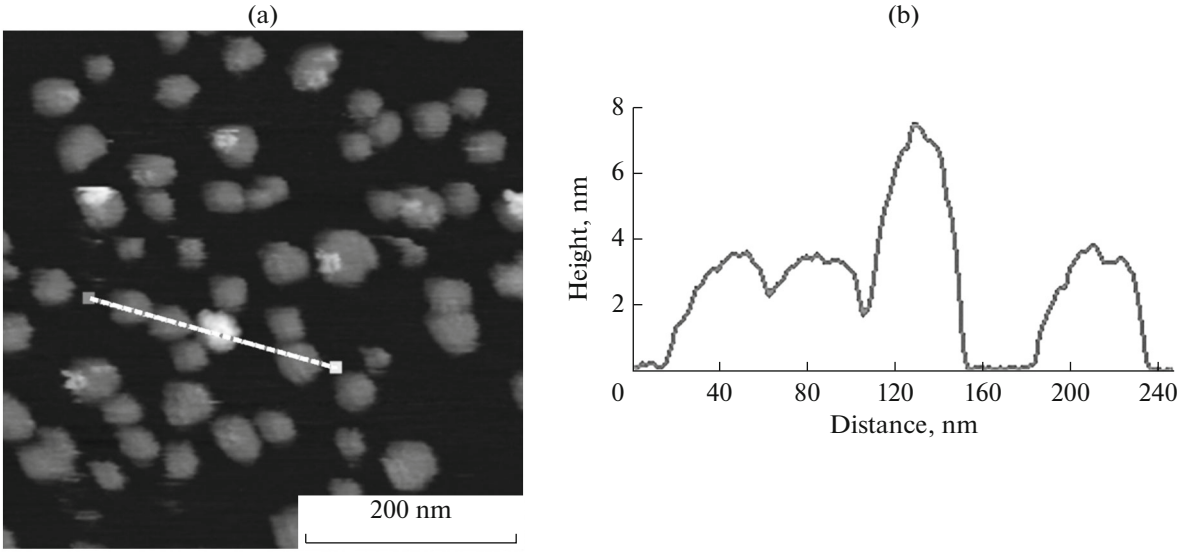

Fig. 6. AFM image of the lipodisc nanoparticles. A section profile is shown on the right.

ter of nanoparticles in solution versus the size of the projected area of the surface-adsorbed nanoparticles.

AFM was used to measure the thickness of the lipodisc nanoparticles according to a protocol which was shown to be suitable for nanodiscs [40–42]. An AFM image of the lipodisc nanoparticles is shown in Fig. 6. The mean height of the empty lipodisc nanoparticles was 3.3±0.3 nm. This value is less than the expected lipid bilayer thickness (4–5 nm). Seemingly, the lipodisc nanoparticles were either flattened at the surface and/or compressed by the tip-sample interaction force. Both effects would decrease the measured height.

The height of some lipodisc nanoparticles was twice as large as others, an example of such object is shown in Fig. 6 together with a section profile. Presumably, it is a pair of stacked lipodisc nanoparticles.

The lateral size of the lipodisc nanoparticles measured by AFM exceeded 23 nm, which was due to the well-known tip broadening effect. We used silicon nitride cantilevers with the curvature radius of up to 20 nm, according to the manufacturer. The tip broadening can be decreased by using supersharp tips with 1–3 nm radius.

We failed to obtain reproducible AFM images of *Np*SRII/*Np*Htr$_{157}$ in lipodisc nanoparticles because the lipodisc nanoparticles were severely dragged by the

cantilever. This problem can be solved in future by optimisation of the buffer composition (pH and ionic strength) and the substrate modification to optimize the tip-sample interaction.

We may estimate the number of lipid molecules that make up a lipodisc nanoparticle. The copolymer has to shield the side surface of the hydrophobic lipid tails from contact with water molecules in order to stabilize the lipodisc nanoparticles. The thickness of the hydrophobic part of the membrane is less than the total thickness of a lipid bilayer. In this work we used the polar lipid extract of *Escherichia coli* membranes, which is mostly composed of lipids containing saturated fatty acid with 16 carbon atoms in the hydrocarbon section [43]. The thickness of the hydrophobic part of the membrane constructed of such lipids h_{hp} is 2.6 ± 0.1 nm [44].

Let us regard a lipodisc nanoparticle as a disc of a lipid bilayer surrounded by the copolymer. In this model we can estimate the copolymer volume as

$$V_{SMA} = \pi R_{LD}^2 h_{hp} - \pi R_{lip}^2 h_{hp},$$

where R_{LD} is the radius of the lipodisc nanoparticle, R_{lip} is the radius of the lipid part. In this study we used a copolymer with a number average molecular weight of 3800, corresponding to ~27 units of styrene and 9 units of maleic acid (molar ratio 3 : 1). Van der Waals volume of this copolymer is $V_{VDV} \sim 3.7$ nm^3 calculated with the Molinspiration Property Calculation Service (www.molinspiration.com). However, the actual amount of space occupied by the polymer should be greater due to loose packaging and hydration of the copolymer:

$$V_{SMA} = \alpha N V_{VDV},$$

where N is the number of copolymer molecules per one lipodisc nanoparticle, α is the volume coefficient describing the differences between the actual and VDW volume. On this basis the number of lipid molecules in a single lipodisc nanoparticle can be estimated as

$$N_{lip} = \frac{2\pi R_{LD}^2}{S_{lip}} - \frac{2\alpha N V_{VDW}}{S_{lip} h_{hp}},$$

where $S_{lip} = 0.66$ nm^2 is the area per one lipid [44]. This formula takes into account that a lipodisc nanoparticle has two sides.

According to the TEM measurements the average radius of a lipodisc nanoparticle is 7.5 nm. The contour length of used SMA copolymer molecule is approximately 9.3 nm (in the approximation of bond lengths and angles of alkanes), which is shorter than the lipodisc nanoparticle circumference (~47 nm). Thus we assume that lipodisc nanoparticles comprise 5 or more SMA molecules per particle.

We can estimate the variation of the amount of lipid molecules per lipodisc nanoparticle with $R_{LD} = 7.5$ nm from the amount of SMA molecules, given the coefficient $\alpha = 1.5$: $N_{lip} = 502$ at $N = 5$, $N_{lip} = 470$ at $N = 10$, $N_{lip} = 406$ at $N = 20$. Comparison of these numbers with the literature data (180–200 lipid molecules per DMPC lipodisc nanoparticle with $R_{LD} = 6$ nm [18]) confirms the assumption that several SMA molecules are needed to stabilize a single lipodisc nanoparticle. For comparison, a nanodisc formation requires two apolipoprotein A (or its recombinant analog MSP) molecules [13, 14]. Contrary to the nanodiscs, there is no reason to expect that the number of SMA molecules in a lipodisc nanoparticle is constant.

Comparison of our results with the available published data is shown in the Table. As noted above, AFM has not been used previously to investigate lipodisc nanoparticles. As follows from the Table, TEM and DLS, when both are used to measure the size of lipodisc nanoparticles, usually provided compatible size values.

The data presented show that lipodisc nanoparticles can be used as monodisperse nanosized carriers for membrane proteins. In the XFEL experiments the information about the size of the studied objects is inevitably lost [45]. In the diffraction experiments, this information corresponds to X-ray photons that have small diffraction angles. In XFEL experiments they are almost impossible to detect near the main beam. It is essential to know this information about the particle size and shape for initial model building. Thus, when the nanodiscs or lipodisc nanoparticles are used as carriers for proteins in structural experiments by XFEL, the information about their size should be obtained by some independent analytical techniques, such as dynamic light scattering, TEM and AFM. The first of these methods is the fastest one, it is used mainly to control the assembly of the lipodisc nanoparticles. TEM is the most flexible of these methods; furthermore, both TEM with negative staining and cryo-TEM can be used not only to measure the size, but also for the construction of the three-dimensional electron density distributions for the analysis of protein structure stabilized in lipodisc nanoparticles [46, 47].

In this paper we used lipodisc nanoparticles to stabilize the photosensitive protein complex *Np*SRII/*Np*HtrII$_{157}$. According to TEM, both empty lipodisc nanoparticles and the lipodisc nanoparticles containing the complex *Np*SRII/*Np*HtrII$_{157}$, have the same average size 15 ± 3 nm, with distribution mode in the range of 12.8–13 nm. It is close to the value obtained by dynamic light scattering (~10 nm).

We have shown that lipodisc nanoparticles can be investigated by AFM, by analogy to nanodiscs [40, 48, 49]. However, the measured thickness of the lipodisc nanoparticles (3.3 ± 0.3 nm) was smaller than the expected thickness of the lipid bilayer (4–5 nm), which could be due to the deformation of the lipodisc nanoparticles by the compressive force executed by the cantilever.

Comparing experimental data with the available data on the lipodisc nanoparticles

The lipid composition and SMA	The incorporated protein	Link	DLS	TEM	Comments
E. coli extract, SMA 3 : 1	*Np*SRII/*Np*HtrII$_{157}$	This work	~10 nm	15 ± 3 nm	The first visualization of lpodisc nanoparticles by AFM
DPPC, SMA 3 : 1 and 2 : 1	Bacteriorhodopsin (bR) and palmitoyltransferase PagP	[22]	Mean size 9.0±1.1 nm for bR in lipodisc nanoparticles and 11.0±1.4 nm for PagP in lipodisc nanoparticles	The size of bR in lipodisc nanoparticles 10.2 nm	Approximately ~11 lipid molecules per one bR molecule.
Lipid mixtures from several cell lines: HEK, High Five, *Saccharomyces cerevisiae* and H69AR, SMA 3 : 1 and 2 : 1	Several ATP-binding-cassette transporters	[46]	–	Cryo-TEM was used. A 3D model of Pgp (P-glycoprotein; ABCB1) was obtained.	Approximately ~17 lipid molecules per one Pgp molecule.
POPC/POPG at 9 : 1 composition, SMA 3 : 1	Empty lipodisc nanoparticles were studied	[16]	The size depends on the proportion of the lipid and SMA, minimum 15 nm	TEM was used to confirm the DLS data	
DMPC, SMA 3 : 1	Empty lipodisc nanoparticles were studied	[15]	Mean size 9 nm	Mean size 9 nm, range 5–15 nm	
DMPC, SMA 3 : 1.	Bacteriorhodopsin (bR)	[18]	Mean size 12±2 nm	–	An empty lipodisc nanoparticle consists of 180–200 lipid molecules.
E. coli lipid extract (from the lysed cells), SMA 2000, 2 : 1	KcsA – tetrameric potassium channel from *Streptomyces lividans,* expressed in *E.coli*	[21]	–	Mean size 10 ± 2 nm	
E. coli lipid extract (from the lysed cells), SMA3000, 3 : 1	ETK-FL – a protein with an incorporated 19F label. ETK stands dor *E. coli* tyrosine kinase.	[17]	–	At low SMA concentration the size was 100 nm. At reasonable SMA concentration the size was 10–20 nm.	–
Lipids from the mitochondrial membranes of *Saccharomyces cerevisiae*, SMA 3 : 1	Proteins from the inner mitochondrial membrane, particularly Complex IV (cytochrome C oxidase)	[20]	–	A monodisperse fraction was chosen by GPC, mean size ~12 nm	
DMPC, SMA 2 : 1	Empty lipodisc nanoparticles were studied	[23]	–	Bimodal size distribution maxima at 11.1 ± 3.3 nm and 16.0 ± 3.0 nm	Small-angle neutron scattering provided 9.8 nm size
E. coli lipid extract (from the lysed cells), SMA not indicated	AcrB protein from *E.coli* – antiporter responsible for efflux of some drugs	[47]	–	A 3D model of AcrB was obtained.	

As shown in the Table, so far the lipodisc nanoparticles have been used for the stabilization of only a few membrane proteins. At the same time, nanodiscs and lipodisc nanoparticles are recognized as valuable tools for structural biology, so we expect that their popularity will grow.

The estimation of the molecular dimensions of the SMA copolymer and the lipids shows that each lipodisc nanoparticle should involve several SMA molecules. This should be further confirmed by experiments and molecular dynamics simulations which are currently on the way.

The reported study was funded by RFBR (research project no. 15-54-12385) and DFG (STE640/14).

REFERENCES

1. M. M. Waldrop, Nature **505**, 604 (2014).
2. J. Hajdu, Curr. Opin. Struct. Biol. **10**, 569 (2000).
3. H. N. Chapman, P. Fromme, A. Barty, et al., Nature **470**, 73 (2011).
4. K. V. Shaitan, M. P. Kirpichnikov, V. S. Lamsin, et al., Vastn. RFFI **4**, 38 (2014).
5. A. Deniaud, E. Moiseeva, V. Gordeliy, et al., in *Membrane Protein Structure Determination*, Ed. by J.-J. Lacapere (Humana Press, 2010), pp. 79–103.
6. V. Cherezov, Curr. Opin. Struct. Biol. **21**, 559 (2011).
7. U. Weierstall, J. C. Spence, and R. B. Doak, Rev. Sci. Instrum. **83**, 035108 (2012).
8. R. Fung, V. Shneerson, D. K. Saldin, et al., Nat. Phys. **5**, 64 (2009).
9. A. Barty, J. Kupper, and H. N. Chapman, Annu. Rev. Phys. Chem. **64**, 415 (2013).
10. K. V. Shaitan, G. A. Armeev and A. K. Shaitan, Biophysics (Moscow) **61** (2), 177 (2016).
11. J. A. Whiles, R. Deems, R. R. Vold, et al., Bioorg. Chem. **30**, 431 (2002).
12. M. Jamshad, Y. P. Lin, T. J. Knowles, et al., Biochem. Soc. Trans. **39**, 813 (2011).
13. J. Borch and T. Hamann, Biol. Chem. **390**, 805 (2009).
14. T. H. Bayburt and S. G. Sligar, FEBS Lett. **584**, 1721 (2010).
15. M. C. Orwick, P. J. Judge, J. Procek, et al., Angew. Chem. Int. Ed. **51**, 4653 (2012).
16. R. F. Zhang, I. D. Sahu, L. S. Liu, et al., Biochim. Biophys. Acta – Biomembranes 1848, 329 (2015).
17. D. Li, J. Li, Y. L. Zhuang, et al., Protein Cell **6**, 229 (2015).
18. M. Orwick-Rydmark, J. E. Lovett, A. Graziadei, et al., Nano Lett. **12**, 4687 (2012).
19. D. Yu, Honors Scholar Theses 316 (2013).
20. A. R. Long, C. C. O'Brien, K. Malhotra, et al., BMC Biotechnol. **13** (2013).
21. J. M. Dorr, M. C. Koorengevel, M. Schafer, et al., Proc. Natl. Acad. Sci. U. S. A. **111**, 18607 (2014).
22. T. J. Knowles, R. Finka, C. Smith, et al., J. Am. Chem. Soc. **131**, 7484 (2009).
23. M. Jamshad, V. Grimard, I. Idini, et al., Nano Res. **8**, 774 (2015).
24. E. N. Lyukmanova, Z. O. Shenkarev, A. S. Paramonov, et al., J. Am. Chem. Soc. **130**, 2140 (2008).
25. Z. O. Shenkarev, E. N. Lyukmanova, A. S. Paramonov, et al., J. Am. Chem. Soc. **132**, 5628 (2010).
26. A. Z. Kijac, Y. Li, S. G. Sligar, et al., Biochemistry **46**, 13696 (2007).
27. E. P. Gogol, N. Akkaladevi, L. Szerszen, et al., Prot. Sci. **22**, 586 (2013).
28. I. Orban-Glass, N. Voskoboynikova, K. B. Busch, et al., Biochemistry **54**, 349 (2015).
29. A. Royant, P. Nollert, K. Edman, et al., Proc. Natl. Acad. Sci. U. S. A. **98**, 10131 (2001).
30. H. Luecke, B. Schobert, J. K. Lanyi, et al., Science **293**, 1499 (2001).
31. V. I. Gordeliy, J. Labahn, R. Moukhametzianov, et al., Nature **419**, 484 (2002).
32. J. P. Klare, I. Chizhov, and M. Engelhard, Results Probl. Cell Differ. **45**, 73 (2008).
33. A. A. Wegener, I. Chizhov, M. Engelhard, et al., J. Mol. Biol. **301**, 881 (2000).
34. V. D. Trivedi and J. L. Spudich, Biochemistry **42**, 13887 (2003).
35. I. P. Hohenfeld, A. A. Wegener, and M. Engelhard, FEBS Lett. **442**, 198 (1999).
36. N. Mennes, J. P. Klare, I. Chizhov, et al., FEBS Lett. **581**, 1487 (2007).
37. K. Shimono, M. Iwamoto, M. Sumi, et al., FEBS Lett. **420**, 54 (1997).
38. C. A. Schneider, W. S. Rasband, and K. W. Eliceiri, Nat. Methods **9**, 671 (2012).
39. J. Kriegsmann, M. Brehs, J. P. Klare, et al., Biochim. Biophys. Acta **1788**, 522 (2009).
40. C. D. Blanchette, J. A. Cappuccio, E. A. Kuhn, et al., Biochim. Biophys. Acta – Biomembranes 1788, 724 (2009).
41. T. H. Bayburt, J. W. Carlson, and S. G. Sligar, Langmuir **16**, 5993 (2000).
42. T. H. Bayburt and S. G. Sligar, Proc. Natl. Acad. Sci. USA. **99**, 6725 (2002).
43. H. G. Yuk and D. L. Marshall, Appl. Environ. Microbiol. **69**, 5115 (2003).
44. B. A. Lewis and D. M. Engelman, J. Mol. Biol. **166**, 211 (1983).
45. S. Marchesini, H. He, H. N. Chapman, et al., Phys. Rev. B 68 (2003).
46. S. Gulati, M. Jamshad, T. J. Knowles, et al., Biochem. J. **461**, 269 (2014).
47. V. Postis, S. Rawson, J. K. Mitchell, et al., Biochim. Biophys. Acta – Biomembranes. 1848, 496 (2015).
48. T. H. Bayburt and S. G. Sligar, Prot. Sci. **12**, 2476 (2003).
49. B. A. Chromy, E. Arroyo, C. D. Blanchette, et al., J. Am. Chem. Soc. **129**, 14348 (2007).